http://dx.doi.org/10.17159/2411-9717/2018/v118n12a3

Ethylenediamine-funtionalized ion exchange resin for uranium recovery from acidic mixed sulphate-chloride media: initial column loading studies

by J.T.M. Amphlett*, C.A. Sharrad*, R.I. Foster*†, and M.D. Ogden‡

Synopsis

A renewed interest in nuclear power around the world in order to reduce greenhouse gas emissions is going to increase demand for uranium as fuel. This will result in more uranium being mined, which will in turn increase associated environmental pressures, such as fresh water use. A move to lower quality waters containing impurities such as chloride would help alleviate these pressures. In this work, we determined the uptake characteristics of weakly basic anion exchange resin Ps-EDA towards uranium from saline solutions in a dynamic flow column. Breakthrough curves were produced, with suppression of uptake being observed for chloride concentrations above 5 g L^{-1}. Calculated resin saturation capacities at zero and 5 g L^{-1} chloride are comparable with literature values for strong-base anion exchange resins, and exceed those published for weak-base resins up to 20 g L^{-1} chloride. Data has been fitted to multiple breakthrough models, with the modified dose-response model most effectively predicting uranium recovery. The results show that the ethylenediamine functionality could be suitable for use in future uranium processing flow sheets where a high-saline lixiviant is used.

Keywords
uranium, ion exchange, chloride media, water quality.

Introduction

Ion exchange (IX) is a key technology in the uranium mining industry and is well established for the extraction of uranium from both acidic and alkaline leach liquors (Edwards and Oliver, 2000). It was first employed in 1952 at the West Rand mine in South Africa (Ford, 1993; Taylor, 2016). H_2SO_4 and Na_2CO_3 are the most commonly employed lixiviants used to solubilize uranium in acidic and alkaline leach conditions respectively. The chemistry of these systems causes uranium to form anionic sulphate or carbonate complexes, which can be taken advantage of by anion exchange resins.

Another major technology for the extraction and purification of uranium from leach liquors is solvent extraction (SX). This technique involves the extraction of uranium from the aqueous phase into an immiscible organic layer. Although this is a commonly used method, there are major drawbacks to it, including the use of large volumes of flammable solvents, solvent loss, phase disengagement, third phase formation, and the production of problematic degradation products (Veliscek-Carolan, 2016). These problems can be circumvented through the use of IX resins.

Strong-base anion (SBA) resins have been the staple choice in both sulphate- and carbonate-based uranium processing circuits, due to their wide pH operating window and high loading capacities (Ogden *et al.*, 2017). These resins are able to overcome the challenges associated with SX, and have an enhanced ability to preconcentrate aqueous metal species. They contain quaternary amine functionality and readily extract anionic species from aqueous solution. However, SBA resins suffer from impaired performance in the presence of iron, which also forms anionic sulphate species ($[Fe(SO_4)_2]^-$ at pH < 3 and high sulphate) and chloride, which cause the suppression of uranium uptake (Moon *et al*, 2017; Ogden *et al.*, 2017).

A significant proportion of the world's uranium resources are located in arid regions such as Australia, Namibia, and South Africa (Nuclear Energy Agency and International Atomic Energy Agency, 2016). As uranium production is a fresh water-intensive process, environmental conflicts can arise, which will surely be exacerbated by an increased uranium demand due to the building of new nuclear reactors (IAEA, 2016). However, not only are there environmental issues surrounding water usage, there are economic ones as well. Any fresh water used in the production of uranium will need to be cleaned and/or recycled, which is an energy-intensive and therefore expensive process. Both of these issues could be

* *School of Chemical Engineering and Analytical Science, The University of Manchester, UK.*
† *Decommissioning Technology Research Division, Korea Atomic Energy Research Institute, Daejeon, Republic of Korea.*
‡ *Separations and Nuclear Chemical Engineering Research (SNUCER), Department of Chemical and Biological Engineering, The University of Sheffield, UK.*
 ISSN 2225-6253. Paper received Nov. 2017; revised paper received Apr. 2018.

surmounted by the use of either seawater or untreated bore water. These water sources are generally of lower quality due to the high levels of aqueous contaminants, especially chloride. Traditional uranium processing flow sheets struggle to perform under such conditions, as discussed above, and it has been observed that chloride levels as low as 2.5 g L^{-1} reduce uranium extraction by 20% (Ogden *et al.*, 2017).

Weak-base anion (WBA) exchange resins have shown a higher selectivity for uranium over iron in sulphate media, as well as an increased tolerance to dissolved chloride (Kunin *et al.*, 1969; Lunt *et al.*, 2007; Mcgarvey and Ungar, 1981; Moon *et al.*, 2017; Ogden *et al.*, 2017; Riegel and Schlitt, 2017). This makes them promising candidates for implementation in future uranium extraction processes which use lower quality water sources. They are considered to be more selective than SBA resins for uranium, equally selective as direct SX, and less selective than a combined IX/SX process such as Eluex/Bufflex (Lunt *et al.*, 2007). WBA resins can contain piridyl, polyamine, and polyamide functionalities, among others (Mcgarvey and Ungar, 1981). However, WBA resins are not suited for use in carbonate systems and are therefore restricted to use in liquors with pH values between 0 and 8.

This work has focused on the ability of an in-house produced WBA resin, Ps-EDA (Figure 1, Table I) to extract uranium from sulphate media in a dynamic flow column at various flow rates and chloride levels. Batch equilibrium studies of uranium uptake onto this resin have been reported previously (Amphlett *et al.*, 2018). Although there are commercial WBA resins available, and large-scale development of a new resin is costly, we believe that there is still merit in the design and testing of new ones. Firstly, the cost of developing the Ps-EDA resin should not be as high as for others, such as a chelation resin with an exotic functional group, as it is produced from common, cheap chemicals. Secondly, as a WBA resin it has the potential for mass production for global use in uranium processes, and thirdly, it allows for relatively facile tuning of the functionality by increasing the polyamine chain, or further functionalization to explore the fundamentals of WBA/hybrid resin chemistry.

Experimental

Equipment and reagents

All chemicals except uranyl sulphate were purchased from Sigma Aldrich and used as received. Uranyl sulphate was produced from stocks of uranyl nitrate provided by the Centre for Radiochemical Research at the University of Manchester. All solutions were made using deionized water (> 18 MΩ).

Uranyl sulphate production

A known mass of uranyl nitrate was dissolved in deionized water. Sodium hydroxide was added to this, forming a uranyl hydroxide precipitate. This precipitate was filtered off and dissolved in sulphuric acid.

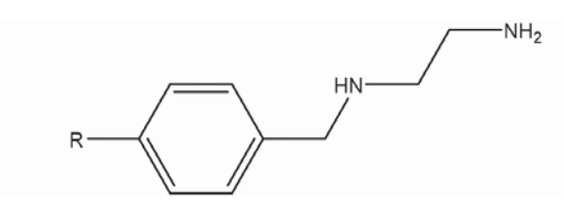

Figure 1—Functionality of Ps-EDA, R represents the polystyrene/DVB resin matrix

Table I

Resin specifications for Ps-EDA

Parameter	Value
Matrix structure	Polystyrene-DVB, macroporous
Functionality	Polyamine (ethylenediamine)
Form	Spherical beads, 16–50 mesh
Cl^- capacity / mg g^{-1}	165.46
UO_2^{2+} capacity / mg g^{-1}	195.96

Effect of flow rate

A uranyl sulphate solution (1 g L^{-1}, pH 2, $[SO_4^{2-}]$ = 0.5 g L^{-1}) was pumped through a column containing 2 mL of wet, settled Ps-EDA resin (1 bed volume, BV) using a Watson-Marlow 323S peristaltic pump. Flow rates of 1.95, 3.75, and 7.5 BV h^{-1} were used. Effluent from the column was collected in multiple fractions using a Bio-Rad model 2110 fraction collector.

Effect of chloride concentration

The same method was used as detailed above; however, the influent flow rate was kept constant at 3.75 BV h^{-1} and chloride (as NaCl) was added to the influent at 5, 10, 20, 30, and 50 g L^{-1}.

Sample analysis

Samples were analysed for uranium concentration using UV/Vis spectroscopy via the Arsenazo(III) method (Wang *et al.*, 2009).

Results

Effect of flow rate on breakthrough performance

Breakthrough curves were produced by plotting C/C_i *vs.* BV (Figure 2) where C is the effluent uranium concentration and C_i is the influent uranium concentration. These curves allow for a qualitative understanding of the effect of flow rate on

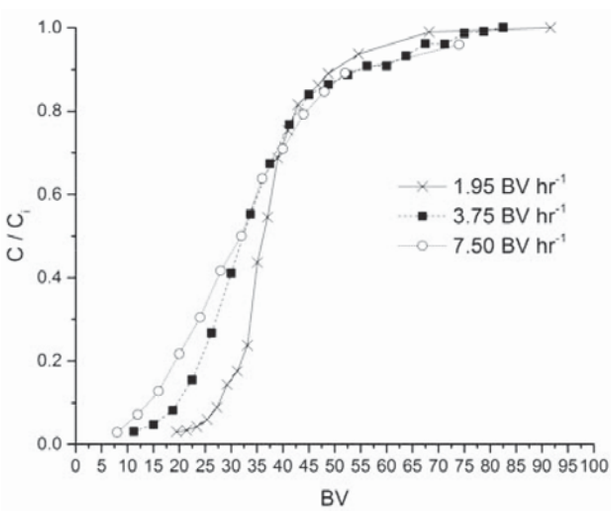

Figure 2—Breakthrough curves for a uranyl sulphate solution (1 g L^{-1}, pH 2) being pumped over 2 mL_{wsr} of Ps-EDA at flow rates of 1.95, 3.75, and 7.5 BV/h^{-1}

Table II

Calculated uptake parameters for the column loading of UO_2^{2+} onto Ps-EDA with increasing flow rate

Flow rate (BV h^{-1})	*Bv* (BV)	B_{cap} (mg)	B_{conc} (mg L^{-1})	t_{50} (min)	B_{50} (BV)	q_m (mg g^{-1})
1.95	19.5	38.56	30.08	1119.38	36.38	98.27
3.75	11.25	21.97	30.25	522.72	32.67	87.17
7.50	8.0	15.59	28.23	251.68	31.46	83.69

uptake behaviour. They also allow for the calculation/identification of certain parameters, such as resin saturation capacity (q_m), breakthrough volume (B_v), breakthrough concentration (B_{conc}), time and volume for 50% breakthrough ($t_{1/2}$ and B_{50}), and breakthrough capacity (B_{cap}) (Table II).

All studied flow rates appear to have achieved saturation of the resin, the point at which no more adsorbate can be taken up and $C = C_i$. However, the volume of influent solution needed to achieve this varies with flow rate. The slowest flow rate (1.95 BV h^{-1}) achieves this with the lowest influent volume, with this volume increasing as flow rate increases. This means that contact time must be increased with increasing flow rates to achieve saturation, which has implications for process scale-up and design.

Breakthrough time (t_{br}) is defined as the point at which effluent adsorbate concentration reaches a set point, which is generally related to its permitted disposal limit (Calero *et al.*, 2009). In these studies, t_{br} shows an inverse trend to that of saturation: as flow rate increases, t_{br} decreases. This shows that the kinetics of uptake are too slow to counteract the increase in flow rate.

Effect of increasing chloride concentration on breakthrough performance

Breakthrough curves were produced from collected data as per the flow rate studies. Data for 0, 5, 10, and 20 g L^{-1} chloride were plotted together (Figure 3), with data for 30 and 50 g L^{-1} being plotted separately for clarity (Figure 4). The 0 g L^{-1} [Cl$^-$] data is taken from the 3.75 BV h^{-1} flow rate experiment. Calculated uptake parameters are presented in Table III.

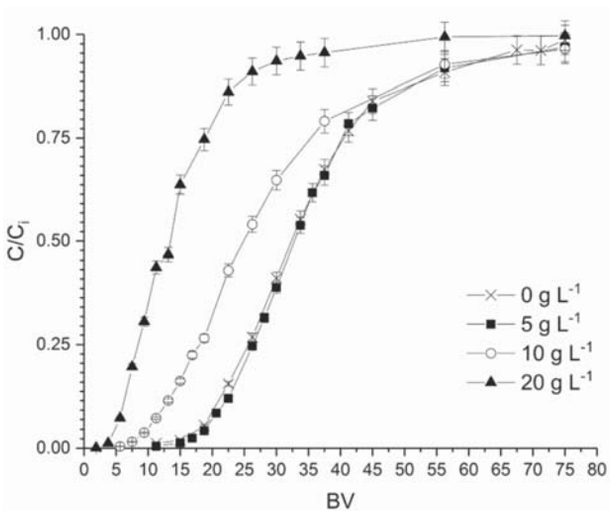

Figure 3—Breakthrough curves for a uranyl sulphate solution (1 g L^{-1}, pH 2) being pumped over 2 mL$_{wsr}$ of Ps-EDA at 3.75 BV h^{-1} with [Cl]$^-$ at 0, 5, 10, and 20 g L^{-1}

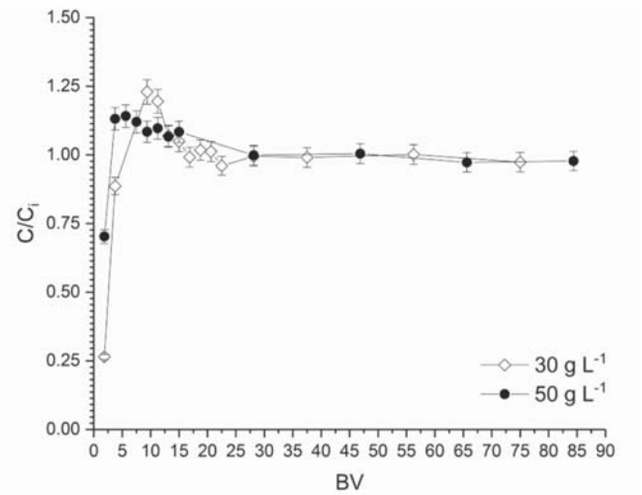

Figure 4—Breakthrough curves for a uranyl sulphate solution (1 g L^{-1}, pH 2) being pumped over 2 mL$_{wsr}$ of Ps-EDA at 3.75 BV h^{-1} with [Cl]$^-$ at 30 and 50 g L^{-1}

No suppression of uranium uptake is seen up to [Cl$^-$] of 5 g L^{-1}, with a decrease in calculated q_m of 74% and 34% for 10 and 20 g L^{-1} respectively. Saturation capacities for 0 and 5 g L^{-1} chloride are within error of each other, suggesting Cl$^-$ has no effect on uranyl loading at concentrations of up to 5 g L^{-1}. Effluents from the 20 and 50 g L^{-1} [Cl$^-$] experiments were upgraded in uranyl compared with the influent concentration.

Discussion

Model fitting

There are multiple models available in the literature which can be used to predict the breakthrough behaviour of ion exchange resins towards aqueous metal species. For the purpose of this work the Adams-Bohart (Bohart and Adams, 1920), Yoon-Nelson (Yoon and Nelson, 1984), Thomas (Thomas, 1944), and modified dose-response (Yan, Viraraghavan, and Chen, 2001) models have been used. It must be noted, however, that these models were not necessarily derived using the theoretical basis of ion exchange chemistry, and therefore the extracted parameters may not be representative of the real experiment. These models primarily allow for comparison with current literature data. All model fitting was carried out via linear regression analysis using Origin Pro 2015, with errors being calculated at a 95% confidence interval from standard errors given by the line of best fit.

Adams-Bohart

The Adams-Bohart model was derived to describe the adsorption of chlorine gas onto charcoal (Bohart and Adams,

Table III

Calculated values of B_v, B_{cap}, B_{conc}, t_{50}, BV_{50}, and q_m for uranium (1 g L^{-1}) loading onto the Ps-EDA resin from pH 2 sulphuric acid with varying concentrations of chloride (5, 10, 20, 30, 40 g L^{-1})

[Cl$^-$] (g L^{-1})	B_v (BV)	B_{cap} (mg)	B_{conc} (mg L^{-1})	t_{50} (min)	BV_{50}	q_m (mg g^{-1})
5	11.250	22.475	4.548	525.568	32.848	88.100 ± 2.983
10	5.625	11.616	4.421	393.168	24.573	62.362 ± 4.055
20	1.875	3.793	0.822	198.928	12.433	28.943 ± 3.484
30*	1.875	3.643	256.848	-	-	-
50*	1.875	3.340	625.946	-	-	-

*It was not possible to calculate t_{50}, BV_{50}, and q_m for [Cl$^-$] of 30 and 50 g L^{-1}.

1920). It assumes that the uptake equilibrium is not instantaneous, with the rate of adsorption being proportional to the residual capacity of the resin (Ansari *et al.*, 2012). This model is generally used to describe the initial section of the breakthrough curve, for $C \leq 0.15C_i$. The linear and nonlinear equations from this model are shown in Equations [2] and [3] respectively, where K_{AB} is the Adams-Bohart constant (L mg^{-1} min^{-1}), t is the contact time (minutes), N_0 is the saturation capacity (mg L^{-1}), Z is the resin bed depth in the column (cm), and v is the influent flow rate (cm min^{-1}).

$$ln\left(\frac{c}{c_i}\right) = K_{AB}C_i t - \frac{K_{AB}N_0 Z}{v} \quad [2]$$

$$\frac{C}{C_i} = \frac{e^{K_{AB}C_i t}}{e^{(K_{AB}N_O Z)/v} - 1 + e^{K_{AB}C_i t}} \quad [3]$$

Goodness of fit (R^2) and model parameters for flow rate and chloride concentration experiments are shown in Tables IV and V, respectively. Due to a sparsity of data at $C \leq 0.15C_i$ for a flow rate of 7.5 BV h^{-1}, collected flow rate data has been fitted to the Adams-Bohart model for $C \leq 0.30C_i$. R^2 values for all [Cl$^-$] apart from 5 g L^{-1} are not acceptable, leading to the conclusion that this model is not able to describe breakthrough in this system. Generally, R^2 values are better in the absence of Cl$^-$, though the only fit with a value above 0.99 was that of 3.75 BV h^{-1}.

Yoon-Nelson

The Yoon-Nelson model was derived to model gaseous adsorption onto solid sorbent respirator cartridges (Yoon and Nelson, 1984). It is based on the assumption that the rate of decrease in the probability of adsorption is proportional to the probability of the adsorbate adsorption and the adsorbate breakthrough on the adsorbent (Calero *et al.*, 2009; Tavakoli *et al.*, 2013). The linear and nonlinear equations for this model are shown in Equations [4] and [5] respectively, where K_{YN} is the Yoon-Nelson constant (min^{-1}).

$$ln\left(\frac{C_i}{C}\right) = K_{YN}t_{50} - K_{YN}t \quad [4]$$

$$\frac{C}{C_i} = \frac{1}{1 + e^{K_{YN}(t_{50} - t)}} \quad [5]$$

Goodness of fit and model parameters for flow rate and chloride concentration experiments are shown in Tables VI and VII, respectively. As with the Adams-Bohart model, R2 values are much better in the absence of chloride. However, in both cases the R^2 values are not adequate. For the chloride

Table IV

Fitting parameters for the Adams-Bohart model at varying flow rates where $C \leq 0.30\ C_i$

Flow rate (BV h^{-1})	R^2	K_{AB} (×10^{-6}) (L mg^{-1} min^{-1})	N_0Z/v (×10^5) (mg min L^{-1})
1.95	0.979	5.35 ± 0.35	12.78 ± 0.84
3.75	0.994	9.39 ± 0.24	5.53 ± 0.36
7.50	0.981	15.66 ± 0.51	2.59 ± 0.55

Table V

Fitting parameters for the Adams-Bohart model at varying [Cl$^-$] where $C \leq 0.30\ C_i$

[Cl$^-$] (g L^{-1})	R^2	K_{AB} (×10^{-5}) (L mg^{-1} min^{-1})	N_0Z/v (×10^5) (mg min L^{-1})
5	0.997	1.93 ± 0.10	4.62 ± 0.11
10	0.860	3.69 ± 12.82	2.67 ± 0.45
20	0.937	6.01 ± 1.74	1.42 ± 0.21

systems, R^2 values are all less than 0.62, showing that this model is unable to effectively model breakthrough in these systems. Predicted time taken to 50% breakthrough does not follow the same trend as calculated from breakthrough data; however, the errors are so large as to bring any conclusion based on this model into question. K_{YN} also shows large errors, further evidencing the inadequacy of this model for this system.

Thomas

The Thomas model was derived to explain column loading of aqueous species onto a zeolite (Thomas, 1944). It is based on the assumption that uptake is controlled not by chemical equilibria, but by mass transfer at the interface between the resin and the aqueous matrix (Calero *et al.*, 2009; Tavakoli *et al.*, 2013). The linear and nonlinear equations from this model are shown in Equations [6] and [7] respectively, where K_{TH} is the Thomas constant (L min^{-1} mg^{-1}), m is the mass of the resin in the column (g), Q is the flow rate (ml min^{-1}), and V_{ef} is the effluent volume (mL).

$$ln\left(\frac{C_i}{C}-1\right)=\left(\frac{K_{TH}}{Q}\right)(q_m m)-\left(\frac{K_{TH}}{q}\right)(C_i V_{ef}) \quad [6]$$

$$\frac{C}{C_i}=\frac{1}{1+e\left(\frac{K_{TH}}{Q}\right)^{(q_m m-c_i v_{ef})}} \quad [7]$$

Model parameters have been extracted from fitting data and are presented in Tables VIII and IX for flow rate and chloride concentration experiments respectively. R^2 values for all data-sets are ≤ 0.98, demonstrating that this model does not adequately describe breakthrough. It also overestimates q_m values compared to those calculated from breakthrough data, though it does predict the same trend in uptake suppression. However, the errors are large enough to prevent reliable conclusions being drawn from the use of this model.

Modified dose-response

The modified dose-response model (Yan *et al.*, 2001) is based on the dose-response model, which has historically been used in the fields of medicine and pharmacology. The linear and nonlinear forms of the equation are shown in Equations [8] and [9] respectively, where a and b are modified dose-response model constants.

$$ln\left(\frac{C_i}{C}-1\right)=a\ln(b)-a\ln(V_{ef}) \quad [8]$$

$$\frac{C}{C_i}=1-\frac{1}{1+\left(\frac{V_{ef}}{b}\right)^a} \quad [9]$$

By equating Equation [9] to 50% removal (C/C_i = 0.5) and applying the Thomas model, it is possible to produce an expression to calculate q_m (Equation [10]). Fitting parameters for this model are shown in Tables X and XI for flow rate and chloride concentration experiments respectively. R^2 values for this model are greater than 0.99 for all data-sets, with no obvious effect of chloride on goodness of fit, and therefore this model is suitable to model column loading. Extracted q_m values are within error of those calculated from breakthrough curve data, though this model tends to overestimate these values. The observed trends for increasing flow rate and suppression by chloride are also predicted by this model. Breakthrough curves for flow rate and chloride data fit with this model are shown in Figures 5 and 6, respectively.

$$q_m=\frac{bC_i}{m} \quad [10]$$

Goodness-of-fit parameters did vary in the presence and absence of chloride. However, both data-sets were in agreement as to which models were and were not able to adequately model breakthrough behaviour, with R^2 values for the modified dose-response model always exceeding 0.99. As breakthrough prediction is consistent when the complexity of the influent matrix is increased, it is reasonable to theorise that uranium breakthrough may be predicted using this model in the presence of other species (such as iron) and for process scale-up.

Table VI

Fitting parameters for the Yoon-Nelson model with varying influent flow rate

Flow rate (BV h^{-1})	R^2	K_{YN} (×10^{-3}) (min^{-1})	t_{50} (min)
1.95	0.980	6.41 ± 0.63	1168.84 ± 27.83
3.75	0.962	6.90 ± 0.57	589.00 ± 17.19
7.50	0.953	1.20 ± 0.74	264.10 ± 19.37

Table VII

Fitting parameters for the Yoon-Nelson model with varying [Cl$^-$]

[Cl$^-$] (g L^{-1})	R^2	K_{YN} (×10^{-3}) (min^{-1})	t_{50} (min)
5	0.616	5.08 ± 1.98	843.19 ± 163.50
10	0.436	5.06 ± 2.98	858.42 ± 328.12
20	0.282	3.52 ± 2.63	717.32 ± 349.51

Table VIII

Fitting parameters for the Thomas model with varying influent flow rate

Flow rate (BV h^{-1})	R^2	K_{TH} (×10^{-6}) (L min^{-1} mg^{-1})	q_m (mg g^{-1})
1.95	0.980	6.48 ± 0.48	102.67 ± 3.09
3.75	0.962	7.16 ± 0.73	96.93 ± 5.99
7.50	0.953	12.27 ± 1.09	87.99 ± 5.89

Table IX

Fitting parameters for the Thomas model with varying [Cl$^-$]

[Cl$^-$] (g L^{-1})	R^2	K_{TH} (×10^{-6}) (L min^{-1} mg^{-1})	q_m (mg g^{-1})
5	0.869	8.86 ± 1.73	103.65 ± 9.12
10	0.814	6.88 ± 1.77	93.80 ± 15.23
20	0.736	8.96 ± 2.68	53.24 ± 16.39

Table X

Fitting parameters for the modified dose-response model with varying influent flow rate

Flow rate (BV h^{-1})	R^2	a	b	q_m (mg g^{-1})
1.95	0.994	8.74 ± 0.43	72.87 ± 0.43	98.42 ± 3.76
3.75	0.998	4.97 ± 0.14	64.59 ± 0.50	86.17 ± 1.98
7.50	0.994	3.39 ± 0.32	60.82 ± 0.51	80.90 ± 2.04

Table XI

Fitting parameters for the modified dose-response model with varying [Cl^-]

[Cl^-] (g L^{-1})	R^2	a	b	q_m (mg g^{-1})
5	0.992	4.97 ± 0.23	67.47 ± 1.59	92.07
10	0.995	3.32 ± 0.13	50.90 ± 1.56	71.80
20	0.992	3.36 ± 0.15	26.40 ± 1.15	36.48

Effect of chloride on uranium recovery

No suppression of uranium uptake onto Ps-EDA is observed for [Cl^-] up to 5 g L^{-1}. This agrees with data collected for uptake onto the bispicolylamine-functionalized WBA resin Dowex M4195 (Ogden *et al.*, 2017), where batch equilibrium studies showed the same trend in uptake suppression with increasing [Cl^-]. Uptake of uranium onto WBA resin Amberlite IRA-67 (tertiary amine functionality) has been assessed for water purification purposes, with saturation capacity determined at 60 mg g^{-1} (Riegel and Schlitt, 2017). This is well below the capacities for uranium uptake onto Ps-EDA at 0 and 5 g L^{-1} chloride and is within an error of q_m for loading from a 20 g L^{-1} chloride solution. Values for saturation capacity are comparable to those determined for a set of SBA resins (81.73–131.81 mg g^{-1}), the staple type for uranium processing circuits (Rychkov, Smirnov, and Gortsunova, 2014).

Above 5 g L^{-1} chloride, suppression of uranium uptake is observed. This is again consistent with work reported in the literature (Moon *et al.*, 2017; Ogden *et al.*, 2017). Ps-EDA extracts uranium via anion exchange; this process can be affected by the presence of other anions in the aqueous matrix, such as chloride. Chloride anions will compete for IX sites on the resin, which will be a contributing factor to the observed reduction in uranium uptake. Another factor to be considered is uranium speciation in mixed sulphate/chloride media. Reported data shows that from 0–6 M chloride there are three different solution species which dominate; $[UO_2(SO_4)_2H_2O]^{2-}$ (0–0.5 M), $[UO_2Cl(SO_4).2H_2O]^-$ (1–2 M), and $[UO_2Cl_4]^{2-}$ (3–6 M) (Moon *et al.*, 2017). As this work was carried out between 0 and 50 g L^{-1} chloride (0–1.4 M) the uranyl-bis-sulfato and the mixed uranyl-chloro-sulfato species will be dominant in solution.

Data for 5, 10, and 20 g L^{-1} chloride produces a traditional breakthrough curve which converges to $C/C_i = 1$. These [Cl^-] (0.14–0.56) correspond to the uranyl-bis-sulfato species being dominant, which is able to outcompete the chloride for IX sites on the resin due to its larger charge (-2 *vs.* -1). The 30 and 50 g L^{-1} chloride (0.85 and 1.41 M) breakthrough curves will have the mixed uranyl-chloro-sulfato species dominating. As the influent solution contacts the resin, chloride is preferentially removed; this process is rapid enough for a solution depleted in chloride to be present within the resin bed, allowing for uranium uptake. This uranium is subsequently eluted off the column by chloride present in the influent solution as resin further 'upstream' of the uranium-loaded resin is already saturated with chloride ions. This process produces an upgraded effluent solution, from 2–20 BV, with C/C_i values reaching 1.25 for the 30 g L^{-1} chloride breakthrough curve. Electrostatics is a key factor in determining what will load onto the Ps-EDA resin. The

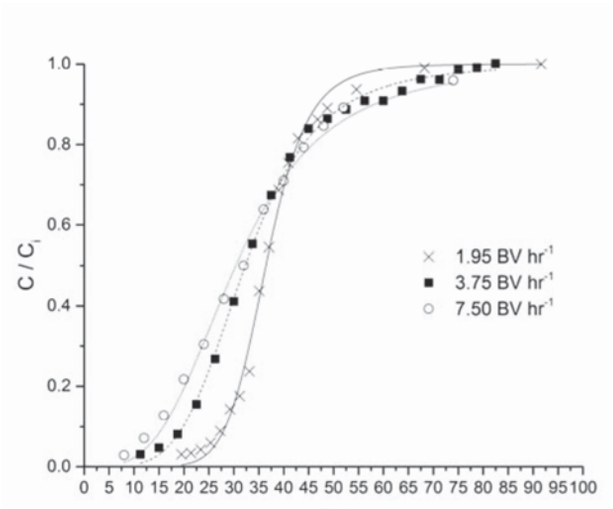

Figure 5—Breakthrough curves for a uranyl sulphate solution (1 g L^{-1}, pH 2) being pumped over 2 mL_{wsr} of Ps-EDA at flow rates of 1.95, 3.75, and 7.5 BV h^{-1} fit with the modified dose-response model

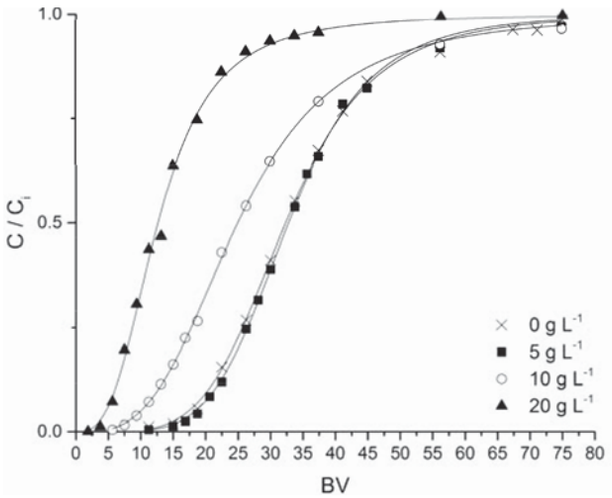

Figure 6—Breakthrough curves for a uranyl sulphate solution (1 g L^{-1}, pH 2) being pumped over 2 mL_{wsr} of Ps-EDA at 3.75 BV h^{-1} with [Cl^-] at 0, 5, 1,0 and 20 g L^{-1} fit with the modified dose-response model

(a) $[R(EDA)(SO_4)] + [UO_2(SO_4)_2H_2O]^{2-} + [Cl]^- \rightarrow [R(EDA)(UO_2(SO_4)_2H_2O)] + [SO_4]^{2-} + [Cl]^-$

(b) $[R(EDA)(SO_4)] + [UO_2Cl(SO_4).2H_2O]^- + 2[Cl]^- \rightarrow [R(EDA)(Cl)_2] + [UO_2Cl(SO_4).2H_2O]^- + [SO_4]^{2-}$

Figure 7—Proposed uptake mechanisms for Ps-EDA in mixed uranium-sulphate-chloride systems at 5, 10, and 20 g L^{-1} chloride (a) and at 30 and 50 g L^{-1} chloride (b)

$[UO_2(SO_4)_2H_2O]^{2-}$ is preferentially sorbed onto the resin compared with monoanionic chloride; however, the more charge-dense chloride outcompetes the relatively large $[UO_2Cl(SO_4).2H_2O]^-$ species at higher chloride concentrations (Figure 7). It has not been determined in this work if preferential uptake would switch to the $[UO_2Cl_4]^{2-}$ species if chloride concentrations were increased above 106 g L^{-1} (3 M).

Conclusions

WBA resin Ps-EDA has been shown to absorb uranium effectively from aqueous sulphate solution at varying flow rates, with an inverse relationship between flow rate and breakthrough time t_{br} , as well as between flow rate and predicted saturation capacity. It has also shown effectiveness for the uptake of uranium from mixed sulphate/chloride media. The presence of chloride in the aqueous phase has a suppressive effect on uranium uptake above 5 g L^{-1} in a dynamic loading column; however, uranium loading capacity at 20 g L^{-1} chloride is comparable to literature values for loading onto WBA resins in the absence of chloride, showing that Ps-EDA is more effective than other available WBA resins for uranium extraction. Loading of uranium from solutions containing $[Cl^-]$ of 30 and 50 g L^{-1} was not possible, with effluent being upgraded in uranium with regards to the influent concentration between 2 and 20 BV.

The modified dose-response model was the only dynamic loading model able to effectively fit the collected data. Modelling produced similar q_m values and showed the same trend in uranium uptake suppression above 5 g L^{-1} chloride. The Adams-Bohart, Yoon-Nelson, and Thomas models all produced inadequate goodness-of-fit parameters, with the Thomas model overestimating q_m values.

The ability of Ps-EDA to outperform other WBA resins for uranium uptake from solutions containing up to 20 g L^{-1} chloride, and loading capacities comparable to SBA resins with solutions containing up to 5 g L^{-1} chloride demonstrate that it is a promising resin for future implementation in uranium recovery processes, potentially replacing SBA resins with a view to more environmentally friendly uranium production. As a WBA resin, Ps-EDA should demonstrate an enhanced tolerance to dissolved iron (Merritt, 1970), a common and problematic contaminant which suppresses uranium uptake (Ogden *et al.*, 2017). Due to the restricted operating pH window, facile elution should be possible using a carbonate solution. Although changing from acidic sulphate to alkaline carbonate media can be expensive, these costs may be offset by removing the need for expensive desalination plants for fresh water production. A caveat to these beneficial properties is that WBA resins are more susceptible to silica fouling than SBA resins (Lunt *et al.*, 2007; Ogden *et al.*, 2017).

Further work on the effect of iron in the aqueous phase needs to be carried out, and is currently under way in our research group, as well as loading experiments from solutions containing > 50 g L^{-1} chloride to look for an increase in uranium uptake. Elution studies also need to be performed. These will fill existing gaps in the literature and establish the potential of Ps-EDA as a candidate IX resin in uranium processing circuits. The EDA functionality can also be readily extended to (hopefully) increase saturation capacity. Scale-up studies also need to be undertaken to assess the validity of the modified dose-response model for predicting column performance as a tool in process design.

Acknowledgements

The authors would like to thank the Centre for Radiochemical Research at the University of Manchester for the provision of uranyl nitrate. This work was funded by the UK Engineering and Physical Sciences Research Council (EPSRC reference: EP/G037140/1).

References

Amphlett, J.T.M., Foster, R.I., Ogden, M.D., and Sharrad, C.A. 2018. Polyamine functionalised ion exchange resins: synthesis, characterisation and uranyl uptake. *Chemical Engineering Journal,* vol. 334. pp. 1361–1370.

Ansari, R., Seyghali, B., Mohammad-Khah, A., and Zanjanchi, M.A. 2012. Highly efficient adsorption of anionic dyes from aqueous solutions using sawdust modified by cationic surfactant of cetyltrimethylammonium bromide. *Journal of Surfactants and Detergents*, vol. 15, no. 5. pp. 557–565. https://doi.org/10.1007/s11743-012-1334-3

Bohart, G.S. and Adams, E.Q. 1920. Some aspects of the behaviour of charcoal with respect to chlorine. *Journal of the American Chemical Society*, vol. 42, no. 3. pp. 523–544. https://doi.org/10.1021/ja01448a018

Calero, M., Hernáinz, F., Blázquez, G., Tenorio, G., and Martín-Lara, M.A. 2009. Study of Cr (III) biosorption in a fixed-bed column. *Journal of Hazardous Materials,* vol. 171, no. 1–3. pp. 886–893.

Edwards, C.R., and Oliver, A.J. 2000. Uranium processing: A review of current methods and technology. *Journal of the Minerals, Metals and Materials Society*, vol. 52, no. 9. pp. 12–20. https://doi.org/10.1007/s11837-000-0181-2

Ford, M.A. 1993. Uranium in South Africa. *Journal of the South African Institute of Mining and Metallurgy*, vol. 93, no. 2. pp. 37–58. https://doi.org/10.1111/j.1813-6982.1953.tb01589.x

IAEA. 2016. Energy, electricity and nuclear power estimates for the period up to 2050. Vienna.

Kunin, R., Gustafson, R.L., Isacoff, E.G., and Fillius, H.F. 1969. Ion exchange resins for uranium hydrometallurgy. *Engineering and Mining Journal*, vol. 170, no. 7. pp. 73–79.

Lunt, D., Boshoff, P., Boylett, M., and El-Ansary, Z. (2007. Uranium extraction: the key process drivers. *Journal of the Southern African Institute of Mining and Metallurgy*, vol. 107, no. 7. pp. 419-426.

Mcgarvey, F.X., and Ungar, J. 1981. The influence of resin functional group on the ion-exchange recovery of uranium. *Journal of the Southern African Institute of Mining and Metallurgy*, vol. 81, no. 4. pp. 93–100.

Merritt, R.C. (1970). The Extractive Metallurgy of Uranium. Colorado School of Mines Research Institute, Golden, CO.

Moon, E.M., Ogden, M.D., Griffith, C.S., Wilson, A., and Mata, J.P. 2017. Impact of chloride on uranium(VI) speciation in acidic sulfate ion exchange systems: Towards seawater-tolerant mineral processing circuits. *Journal of Industrial and Engineering Chemistry*, vol. 51. pp. 255–263. https://doi.org/10.1016/j.jiec.2017.03.009

Nuclear Energy Agency and International Atomic Energy Agency. 2016. Uranium 2016: resources, production and demand. https://doi.org/https://www.oecd-nea.org/ndd/pubs/2004/5291-uranium-2003.pdf

Ogden, M.D., Moon, E.M., Wilson, A., and Pepper, S.E. 2017. Application of chelating weak base resin Dowex M4195 to the recovery of uranium from mixed sulfate/chloride media. *Chemical Engineering Journal*, vol. 317. pp. 80–89. https://doi.org/10.1016/j.cej.2017.02.041

Riegel, M., and Schlitt, V. 2017. Sorption dynamics of uranium onto anion exchangers. *Water*, vol. 9, no. 4. pp. 268-285. https://doi.org/10.3390/w9040268

Rychkov, V.N., Smirnov, A.L., and Gortsunova, K.R. 2014. Sorption of uranium from underground leaching solutions with highly basic anion exchangers. *Radiochemistry*, vol. 56, no. 1. pp. 38–42. https://doi.org/10.1134/S1066362214010081

Tavakoli, H., Sepehrian, H., Semnani, F., and Samadfam, M. 2013. Recovery of uranium from UCF liquid waste by anion exchange resin CG-400: Breakthrough curves, elution behavior and modeling studies. *Annals of Nuclear Energy*, vol. 54. pp. 149–153.

Taylor, A. 2016. Short course in uranium ore processing.ALTA Metallurgical Services.

Thomas, H.C. 1944. Heterogeneous ion exchange in a flowing system. *Journal of the American Chemical Society*, vol. 66, no. 10. pp. 1664–1666.

Veliscek-Carolan, J. 2016. Separation of actinides from spent nuclear fuel: A review. *Journal of Hazardous Materials*, vol. 318. pp. 266–281.

Wang, G., Liu, J., Wang, X., Xie, Z., and Deng, N. 2009. Adsorption of uranium (VI) from aqueous solution onto cross-linked chitosan. *Journal of Hazardous Materials*, vol. 168. pp. 1053–1058. http://ac.els-cdn.com/S0304389409003549/1-s2.0-S0304389409003549-main.pdf?_tid=db49eb3c-04e8-11e7-9517-00000aab0f6candacdnat=1489078561_27ca4f6ee9bdf1a1ccf8d6d550e1b300

Yan, G., Viraraghavan, T., and Chen, M. 2001. A new model for heavy metal removal in a biosorption column. *Adsorption Science and Technology,* vol. 19, no. 1. pp. 25–43.

Yoon, Y.H., and Nelson, J.H. 1984. Application of gas-adsorption kinetics. I. A theoretical-model for respirator cartridge service life. *American Industrial Hygiene Association Journal*, vol. 45, no. 8. pp. 509–516. ◆